The Morphology during Extrusion of PA6/PP Blends in the Presence of Nanoclays

M.F. Almeida [a], A.V. Machado [b] and J.A. Covas [c]

I3N-Institute of Nanostructure, Nanomodelling and Nanofabrication University of Minho, Guimarães, Portugal

[a] maria.ferreira@dep.uminho.pt,

[b] avm@dep.uminho.pt,

[c] jcovas@dep.uminho.pt

Keywords: Nanocomposites, Polymer blends, Melt compounding, Twin screw extruder, Dispersion.

Abstract

The present study investigates the morphology of polyamide (PA6) and polypropylene (PP) blends in the presence of an organoclay during extrusion. Physical PA6 /PP blends and blends of PA6/PP and PP modified with maleic anhydride, both filled with a montmorillonite (MMT) modified alkyl ammonium organoclay, were prepared in a modular co-rotating twin screw extruder. Samples were collected along the extruder and analyzed by X-ray diffraction (XRD), oscillatory rheology, and scanning and transmission electron microscopy (SEM and TEM, respectively). Intercalation and some degree of clay exfoliation seem to have been achieved. Generally, the presence of the organoclay yields a finer dispersed phase along the extruder.

Introduction

Since the pioneering work of researchers at Toyota in the seventies, industrial and scientific interest on nanocomposites has grown dramatically [1-2]. Compounding polymers with small concentrations of organically modified nanoclays may enhance significantly the mechanical and physical properties of the polymers, as well as their processability [3-4]. Research has also been focused on the possibility of using nanoclays both as compatibilizers and nanofillers in immiscible polymer blends [5-7]. In fact, their presence refines the size of the dispersed phase, stabilizes it against coalescence and ensures interfacial adhesion between the two phases, thus improving the final mechanical properties [6, 7]. Hong et. al [8] investigated the effect of the addition of a small amount of organoclay on the morphology of immiscible PBT/PE polymer blends and showed that the size of the dispersed phase decreased with increasing organoclay content. Ray et. al [7] studied the role of organically modified layered silicates as compatibilizers for immiscible PS/PP blends and demonstrated that the silicate layers were located at the interface between the two polymers, resulting in a decrease in interfacial tension and particle size and in a remarkable improvement of the mechanical properties. Similarly, Khatua et. al [9] reported a significant decrease of the dispersed phase of PA6/EPR blends even when only small amounts of organoclay were added. Identical observations were made for PA6/LLDPE blends [10]. The decrease of the particle size of the dispersed phase was explained by these authors by the compatibilization effect of the organoclay. Nonetheless, Dharaiya et. al explained the decrease of the particle size of the dispersed phase of PP/PA blends by the lamellar and fibrilar forms of the blend phases in the presence of organoclays [11].

Despite the practical importance of PA6/PP blends, little has been reported on the effect on their morphology of incorporating organoclays. Moreover, the evolution of the morphology of polymer blends in the presence of organoclays during melt compounding in an extruder is still unknown. Thus, this study aims at examining the evolution of the morphology of PA6/PP blends in the presence of organoclays along a twin screw extruder, TSE, with and without the addition of PP modified with maleic anhydride (PP-g-MA). Samples collected during processing were analyzed by XRD, rheology, and SEM and TEM microscopies.

Materials and experimental procedure

The Polyamide 6, PA6 (DOMAMID 27), manufactured by Atofina, has a melting temperature of approximately $220^{\circ}\mathrm{C}$ and a MFI value between 17 and 23 $\mathrm{g}/10$ min (at $235^{\circ}\mathrm{C}$ and 2.16 kg). The Polypropylene homopolymer, PP (MOPLEN HP502N, from Basell) has a melting temperature around $160^{\circ}\mathrm{C}$ and a MFI value of 12 $\mathrm{g}/10$ min (at $230^{\circ}\mathrm{C}$ and 2.16 kg weight). The PP grafted with maleic anhydride (PP-g- MA) contains 1wt% MA (Orevac CA 100 from Arkema), has a melting temperature of $167^{\circ}\mathrm{C}$ and a MFI of $150\ \mathrm{g}/10$ min (at $230^{\circ}\mathrm{C}$ and 2.16 kg weight). The organoclay, Cloisite 15A (C15A), produced by Southern Clay Products, consists of MMT modified organically with $125\mathrm{meq}/100$ g of quaternary alkylammonium salts.

After drying the PA6 and the nanoclay under vacuum at $80^{\circ}\mathrm{C}$ during $12-16$ hours, they were tumble-mixed with PP or PP-g-MA, in order to obtain the compositions PA6/PP 70/30w/w, PA6/PP/C15A 70/30/5 w/w/w, and PA6/PP/PP-g-MA/C15A 70/30/5/5, w/w/w/w. The materials were processed in a Leistritz LSM 30.34 modular co-rotating intermeshing TSE (with a screw diameter of 30 mm and $\mathrm{L/D}=29$). The barrel was set uniformly at $230^{\circ}\mathrm{C}$, the screw speed at 200 rpm and the feed rate of the gravimetric feeder at 4 kg/h. Fig. 1 illustrates the extruder layout, the screw geometry and the location along the barrel of the sampling devices used to collect material samples from within the extruder during normal extruder operation. These samples were immediately quenched in liquid nitrogen for subsequent characterization. The screws include three intensive mixing zones comprising different series of staggered kneading disks ($12\ \mathrm{KB}+$ a lefthanded element, 4 KB and 3 KB , respectively) with negative angles (-30°) and a 4^{th} mixing zone consisting of a left-handed element (L). Such a high shear intensity screw profile is required to enhance dispersion; the sampling devices are located in these regions, where positive pressure develops.

After surface trimming of the samples, their X-ray diffraction spectra were obtained using a Rigaku Geigerflex XRD equipment operating with $\lambda = 1.54\text{Å}$ and $\mathrm{Cu} - \mathrm{K}\alpha$ radiation (at 40 Kv and 40 mA), the 2θ angles being varied from $1.7°$ to $5°$. Since the linear viscoelastic response of polymer blends and nanocomposites has been considered as a sensitive probe of morphology/degree of dispersion [4, 12, 13], samples were also compression moulded for 10 minutes at $230\ ^\circ\mathrm{C}$ under a pressure of 30 ton, to obtain disks with a diameter of 25 mm and a thickness of 1 mm . These were then subjected to isothermal frequency sweeps from 0.01 to 100 Hz , at $230^\circ\mathrm{C}$, in a TA instruments RG2 oscillatory rheometer, operating with parallel-plate geometry (diameter 25 mm , gap of 0.9 mm). The strain was kept at 1% in order to ensure the required linear viscoelastic response.

The samples to be characterized by SEM (Leica Cambridge S 360) were fractured at low temperature and etched with hot xylene to remove the PP phase. In the case of TEM (Philips CM 120, operating with a voltage of 120 kV), samples with a thickness of less than 100 nm were obtained by cryo-ultramicrotomy (at $-45^\circ\mathrm{C}$, under liquid nitrogen), using a diamond knife and then stained with RuO_4.

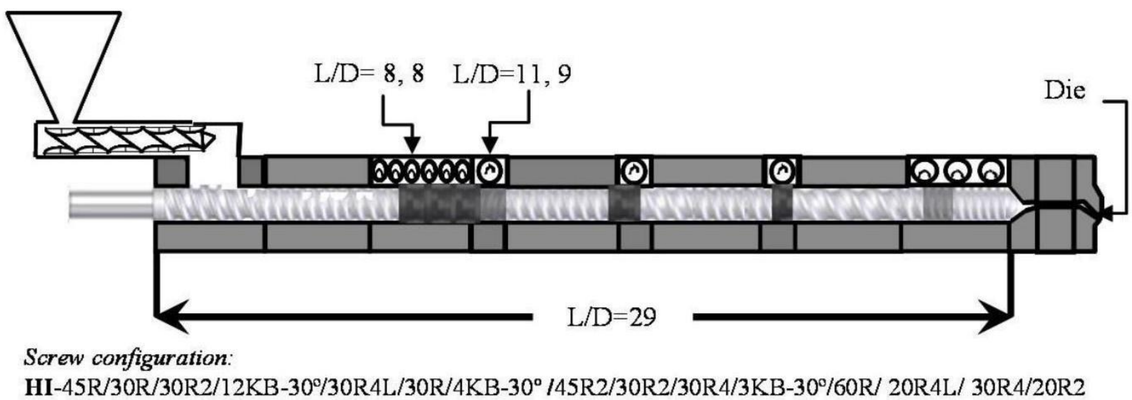

Fig. 1 - Extruder layout, screw configuration and sampling devices

Results and discussion

The X-ray spectra of the samples collected along the extruder for PA6/PP/C15A blends without and with PP-g-MA are shown in Fig. 2. The characteristic peak of the crystalline C15A nanoclay shifts to lower angles as the location of the sample gets closer to the die. Since this indicates an increase of the silicate interlayer distance, it should represent the progressive formation of an intercalated structure. This process is obvious in both blends. At the die no peak can be identified, thus exfoliated silicate layers could also have been formed simultaneously with the intercalated structures.

These observations demonstrate that blends with a relatively well dispersed organoclay can be prepared in conventional compounding twin-screw extruders.

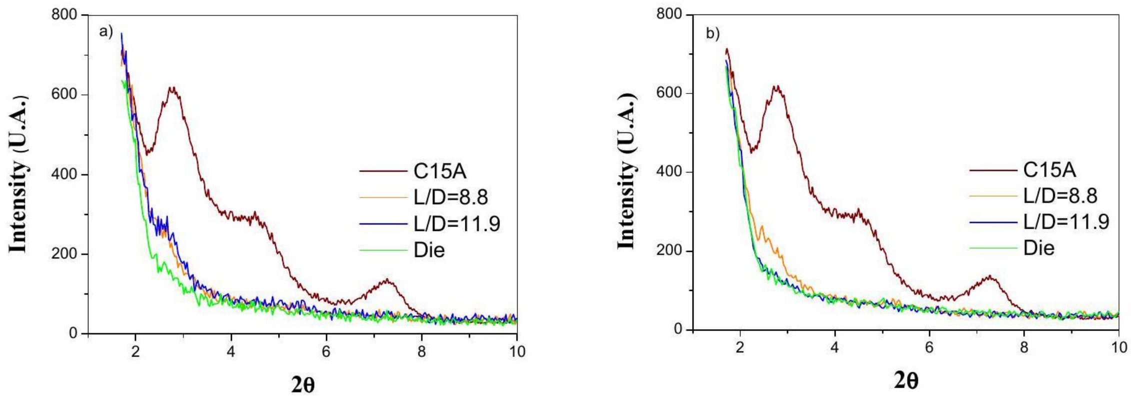

Fig. 2 - X-ray diffraction spectra of samples collected along the extruder: a) PA6/PP/C15A (70/30/5); b) PA6/PP/PP-g-MA/C15A (70/30/5/5).

The rheological response in the linear viscoelastic regimen of nanocomposites (in terms of the storage and loss moduli, G' and G", respectively, and complex viscosity, η^*) has been consistently reported to increase with nanoclay content [12, 13]. A plateau at low frequencies is also generally observed. The curves presented in Fig. 3 (b) for the extrudates are in good agreement with the previous studies, since the values of the rheological parameters of the two blends filled with organoclay are much higher than those of the PA6/PP blend.

Fig. 3 (a) shows the evolution of the same parameters along the screw axis. Since up to $\mathrm{L/D} = 8.8$ melting was not completed, rheological measurements could only be performed for samples collected from $\mathrm{L/D} = 9.4$ onwards. Little, if any, axial evolution can be perceived. This seems to indicate that most of the dispersion takes place upon melting, when high stresses, complex flow patterns and intense surface generation develop.

Given the apparent lack of sensitivity of the rheological measurements to an eventual morphology evolution along the screw, the morphology was directly observed via SEM and TEM. Fig. 4 presents the morphologies present at $\mathrm{L/D} = 8.8$ and 11.9 and at the die for the different blends. The immiscible PA6/PP blend exhibits large dispersed PP particles in a PA6 matrix, due to the immiscibility of the polymers and the consequent high interfacial tension. No axial evolution can be observed. The morphology of the two blends filled with organoclay is quite distinct: not only the morphology is generally finer, but the average particle size decreases towards the die. At the die, the average size of the PP drops is $10{,}0.6$ and 0.3μ m for $\mathrm{PA6/PP}$, $\mathrm{PA6/PP/C15}$ and $\mathrm{PA6/PP/PP-g-MA/C15A}$, respectively. These differences are often associated with the compatibilization effect of the organoclay and PP-g-MA [4-10]. However, the micrographs of Fig. 4 seem to show that compatibilization is more efficient in the presence of PP-g-MA, which could be attributed to the formation of a copolymer between the amine groups of the PA6 and the anhydride groups of the PP-g-MA at the interface [14], resulting in interactions between the blend components that are stronger than those between the nanoclay and the polymers.

The location of the organoclays in the blend can be identified in Fig. 5, as the high resolution of TEM enables the direct observation of the silicate layers [15]. In the case of the PA6/PP/C15 blend, the silicate layers are mainly dispersed in the PA6 phase and only a small amount is located at the interface. Conversely, in the PA6/PP/PP-g-MA/C15A blend the silicate layers are essentially to be found at the interface, between PA6 and PP.

The presence of PP-g-MA, a polar polymer, will improve the interaction of PP with the organoclay.

Given the above, the differences in particle size observed by SEM can be related to the location of the silicate layers: as the amount of organoclay at the interface increases, the particle size of the dispersed phase decreases. The results reported here are in line with previous works attributing a compatibilization effect to the presence of PP-g-MA and also organoclay [4-10]. However, this is still a matter under debate, as the decrease of particle size has also been associated to the lamellar and fibrilar forms of the blend phases in the presence of organoclays (more specifically, the thin fibrils formed upon mixing break-up into smaller droplets due to the hydrodynamic stresses) [15].

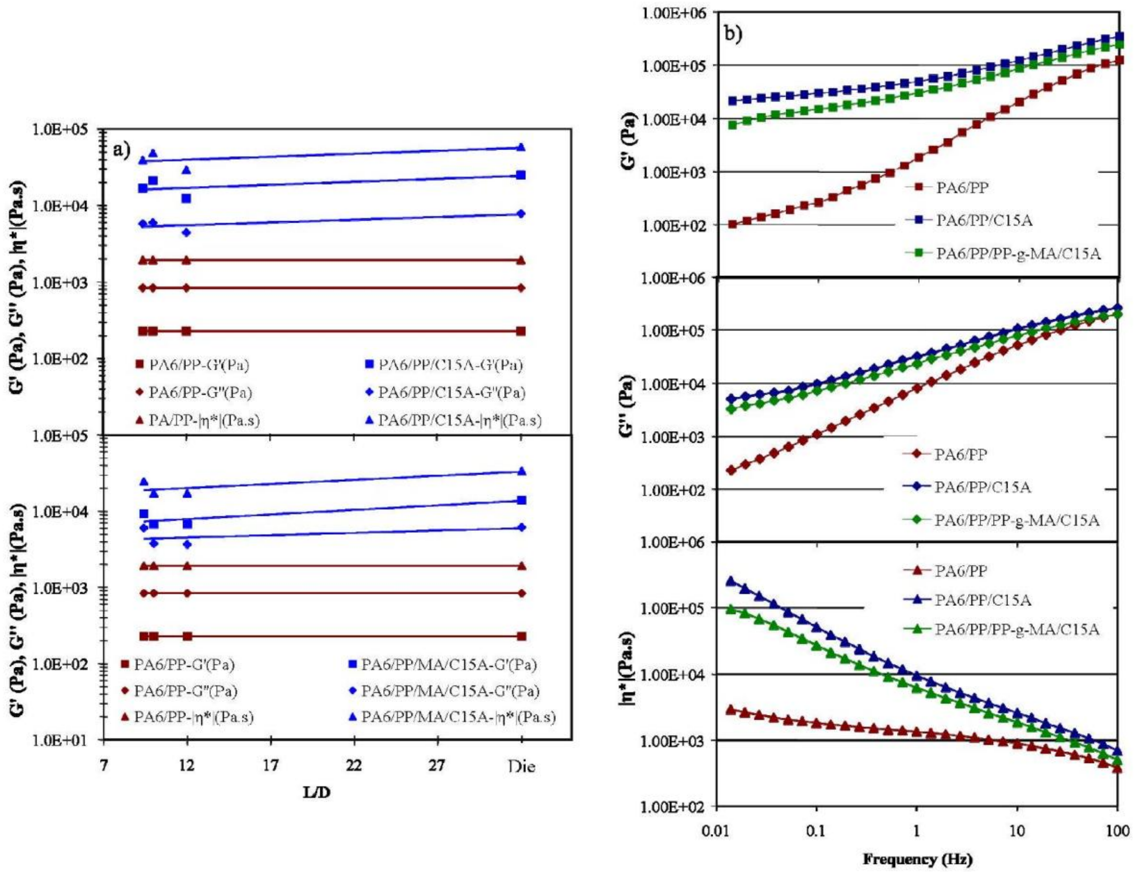

Fig. 3 - G', G'' and $|\eta^*|$ for blends PA6/PP, PA6/PP/C15A and PA6/PP/PP-g-MA/C15A: (a) along the extruder and (b) at the die exit at fixed frequency (0.07 Hz).

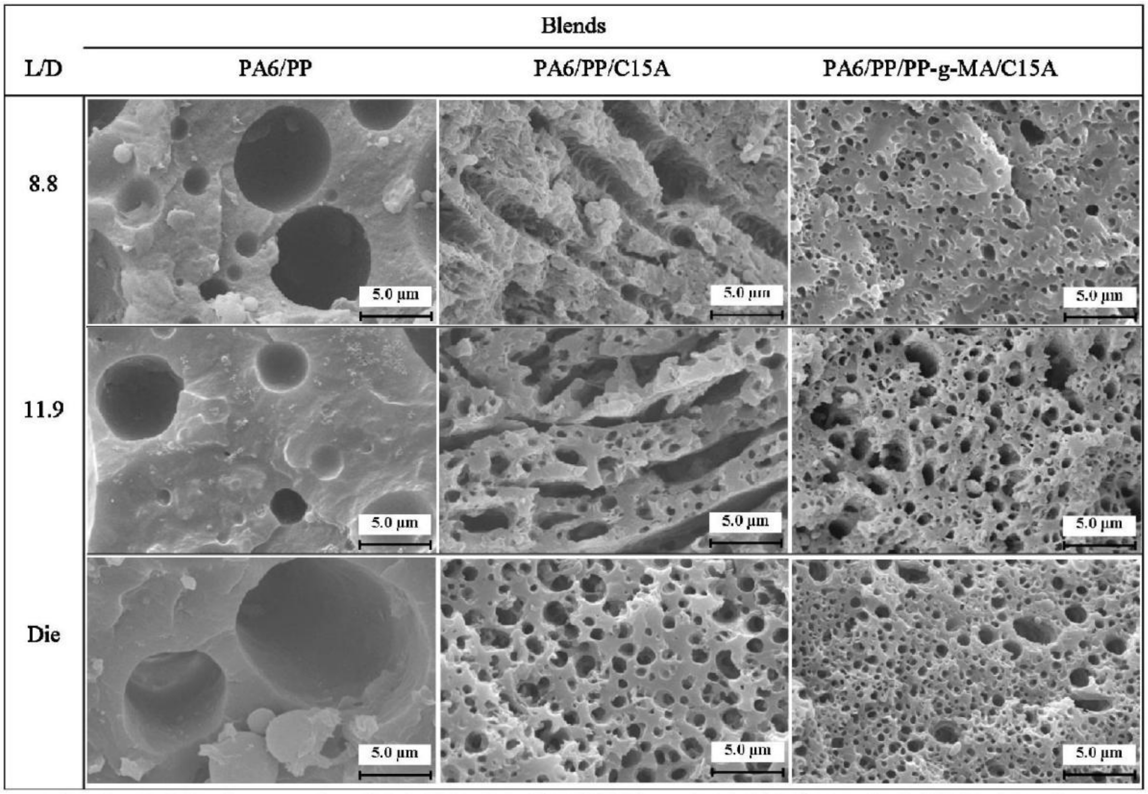

Fig. 4 - SEM micrographs of PA6/PP, PA6/PP/C15A and PA6/PP/PP-g-MA/C15A blends at L/D = 8.8, L/D = 11.9 and die.

Magnificalion		
Blen ds	7100	31000

PA6/ PP/C 15A	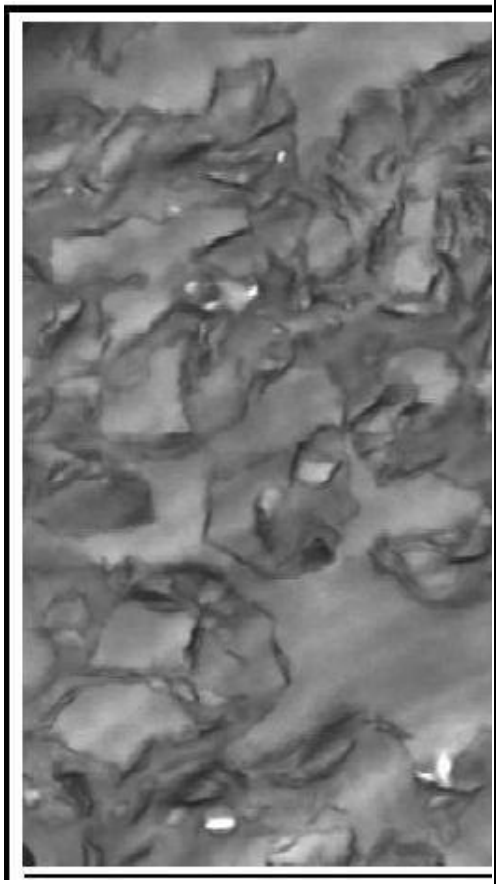	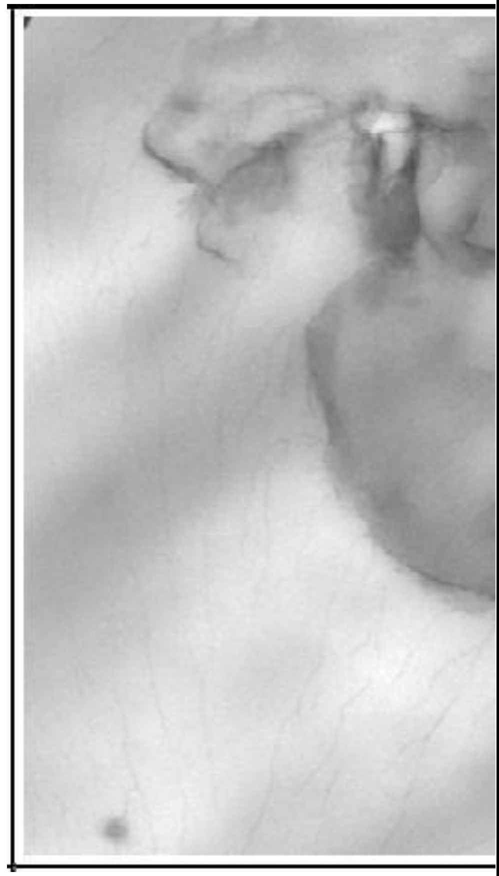

PA6/PP/PP-g-MA/C15A

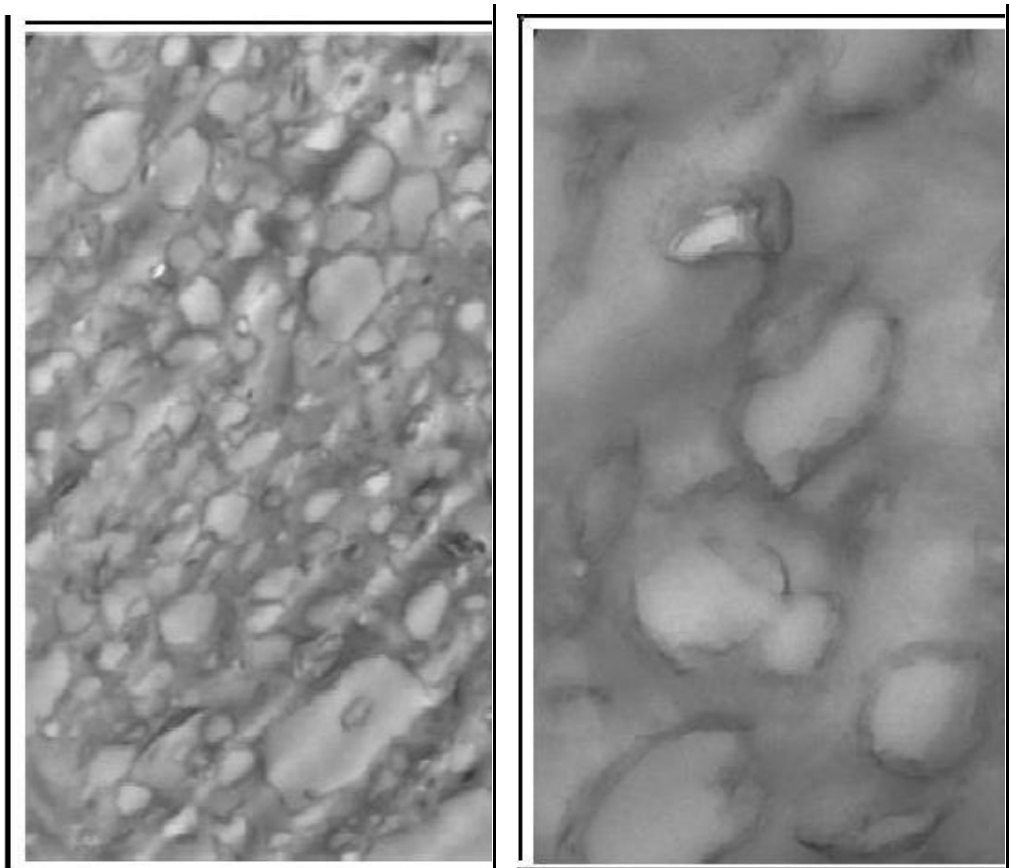

Fig. 5 - TEM micrographs of PA6/PP/C15A and PA6/PP/PP-g-MA/C15A blends (approx. 7100 × and 31000 × magnification).

Conclusions

Melt compatibilized PA6/PP blends were filled with organoclay Closite C15A. Good final dispersion in polymeric matrix was achieved, as indicated by the evidence of intercalation and possible exfoliation provided by XRD. As for the evolution of dispersion along the screw, rheological data could not detected any changes; most probably, this is due to the fact that most of the dispersion developed upon melting, upstream of the location where samples were collected. However, a decrease in particle size of the dispersed phase along the screw could be observed by SEM and TEM. Also it was shown that the organoclays were located either at the interface or dispersed in the matrix depending on the presence of PP-g-MA.

References

[1] G. Ranghino, G. Giannotta, G. Marra and R. Po: Rev. Adv. Mater. Sci. Vol. 5 (2003), p.413.
[2] L. A. Utracki, M. Sepehr and J. Li: International Polymer Processing XXI. Vol. 1 (2006), p. 3.

[3] R. Scaffaro, M.C. Mistretta and F.P. La Mantia: Polymer Degradation and Stability. Vol. 93 (2008), p. 1267.
[4] D.W. Schaefer and R.S. Justice: Macromolecules. Vol. 40 (2007), p. 2.
[5] G. Chen, H. Kim, E. Kim and J. Yoon: Polymer. Vol. 46 (2005), p. 11829.
[6] S. Ray and M. Bousmina: Macromolecules Rapid Communication. Vol. 26 (2005), p. 1639.
[7] S. Ray and M. Bousmina: Polymer. Vol. 46 (2005), p. 12430.
[8] J. Hong, H. Namkung, K. Ahn, S. Lee and C. Kim: Polymer. Vol. 47 (2006), p. 3967.
[9] B. B. Khatua, D. J. Lee, H. Y. Kim and J. K. Kim: Macromolecules. Vol. 37 (2004), p. 2454.
[10] Y. Yoo, C. Park, S. Lee, K. Choi, D. Kim and J. Lee: Macromolecules Chemistry Physics. Vol. 206 (2005), p. 878.
[11] D. P. Dharaiya and S. C. Jana: Journal Polymer Science: Part B: Polymer Physics, Vol. 43 (2005), p. 3638.
[12] W. Lertwimolnun and B. Vergnes: Polymer.Vol. 46 (2005), p. 3462.
[13] S. S. Ray and M. Bousmina: Progress in Materials Science. Vol. 50 (2005), p. 962.
[14] A. V. Machado, J. A. Covas and M. van Duin: Journal of Polymer Science: Part A: Polymer Chemistry. Vol. 37, (1999) 1311-1320
[15] Z. P. Luo and J. H. Koo: Polymer. Vol. 49 (2008), p. 1841